INTERNATIONAL JOURNAL OF
NUMERICAL ANALYSIS AND MODELING
Volume 14, Number 4-5, Pages 604–626

HIGH DEGREE IMMERSED FINITE ELEMENT SPACES BY A LEAST SQUARES METHOD

SLIMANE ADJERID, RUCHI GUO AND TAO LIN

Abstract. We present a least squares framework for constructing p-th degree immersed finite element (IFE) spaces for typical second-order elliptic interface problems. This least squares formulation enforces interface jump conditions including extended ones already proposed in the literature, and it guarantees the existence of p-th IFE shape functions on interface elements. The uniqueness of the proposed p-th degree IFE shape functions is also discussed. Computational results are presented to demonstrate the approximation capabilities of the proposed p-th IFE spaces as well as other features.

Key words. Interface problems, discontinuous coefficients, finite element spaces, curved interfaces, higher order.

1. Introduction

In this manuscript, we present a least squares procedure for constructing higher degree IFE spaces for solving second-order elliptic interface problems of the form

$$-\nabla \cdot (\beta \nabla u) = f, \quad \text{in } \Omega = \Omega^1 \cup \Omega^2, \tag{1a}$$

$$u = g, \quad \text{on } \partial\Omega, \tag{1b}$$

where, without loss of generality, the domain $\Omega \subseteq \mathbb{R}^2$ is assumed to be split by an interface curve Γ into two subdomains Ω^1 and Ω^2. To close the problem we impose the classical jump conditions on the interface

$$[u]_\Gamma \; := \; u^1|_\Gamma - u^2|_\Gamma = 0, \tag{1c}$$

$$\big[\beta \nabla u \cdot \mathbf{n}\big]_\Gamma \; := \; \beta_1 \nabla u^1 \cdot \mathbf{n}|_\Gamma - \beta_2 \nabla u^2 \cdot \mathbf{n}|_\Gamma = 0, \tag{1d}$$

where $\mathbf{n}$ is the unit normal vector to the interface Γ. The diffusion coefficient β is assumed to be a positive piecewise constant function such that

$$\beta(X) = \begin{cases} \beta_1 & \text{for } X \in \Omega^1, \\ \beta_2 & \text{for } X \in \Omega^2. \end{cases}$$

It is well-known that, in both theory and practice, traditional finite element methods can be used to solve interface problems provided that their meshes are body-fitting [4, 9, 12, 40], see an illustration in Figure 1 for a body-fitting mesh. This body-fitting restriction hinders efficient applications of finite element methods in applications where the interfaces evolve because of the involved physics such as in multi-phase fluid simulation [26, 29] or because of computational algorithms such as those for shape optimization problems [7, 22]. Generating a new mesh to fit an evolving interface at each step is not only time consuming, but it can also cause several difficulties such as the need for different finite element spaces on different meshes at different steps. Hence, numerical methods have been developed

Received by the editors on December 31, 2016, accepted on May 3, 2017.
2000 *Mathematics Subject Classification.* 65N5, 65N30, 65N50, 35R05.

that can use interface-independent meshes to solve interface problems by adapting traditional numerical methods for solving partial differential equations. Adaptions or modifications can be loosely categorized into two groups. Methods from the first group employ suitable equations in elements around the interface either in finite difference formulation such as the immersed interface method [28, 31] or in finite element formulation such as the unfitted finite element method based on Nitsche's penalty idea [20, 21]. Methods from the second group use specially constructed local approximation functions on interface elements according to the involved interface jump conditions. Instances of these methods are extended finite element methods (XFEM) [5, 37, 39] and IFE methods [14, 17, 18, 23, 27, 30, 33].

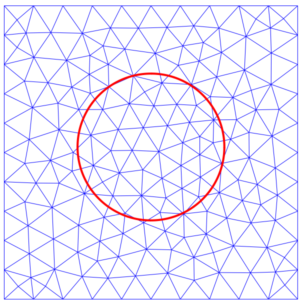

FIGURE 1. An body-fitting mesh and interface.

IFE methods use Hsieh-Clough-Tocher type macro finite element functions [8, 13] on interface elements. For local IFE spaces consisting of piecewise polynomials defined on subelements formed by cutting each interface element with a line approximating the interface, we refer readers to [14, 27, 32, 33] for linear polynomials, [23, 24, 34] for bilinear polynomials and [17, 41] for rotated Q_1 polynomials. All linear and bilinear IFE spaces mentioned above have the optimal convergence rates. Higher degree IFE spaces are desirable since they lead to highly accurate solutions and can be used to design efficient local adaptive h-p refinement algorithms.

Authors in [3, 10, 11, 35] discussed higher degree IFE spaces for 1D interface problems. They considered the extended jump conditions that led to unique construction of the IFE shape functions and optimally convergent IFE spaces. In particular, a p-th degree optimally convergent IFE space was developed in [3]. For 2D interface problems, there are two major obstacles for the development of higher degree IFE spaces. One obstacle is that, on each interface element, a higher degree IFE function can no longer be a macro finite element function piecewisely defined on polygonal subelements because of the intrinsic second-order $\mathcal{O}(h^2)$ limitation of the line. Another obstacle is the proper choice and enforcement of extended jump conditions for determining all the coefficients in each higher degree IFE shape function in piecewise polynomial format such that the resulting IFE space has the optimal approximation capability.

There have been efforts to overcome these obstacles. Recently, several authors [16, 17, 18] have investigated piecewise polynomial shape functions constructed by enforcing jump conditions on the actual interface curve. Even though the involved polynomials are of lower degree such as linear or bilinear, an IFE function in these articles is a piecewise polynomial defined on subelements with the interface as part of their edges, i.e., the subelements to define a local IFE shape function are not polygons. Furthermore, a constant coefficient case was considered by Guzman et al. [19] for arbitrary high degree methods using the correction term idea. For the discontinuous coefficient case, Adjerid et al. [1, 2] considered consistent extended jump conditions that were derived from the regularity assumption of the right hand side f in (1a), and they constructed p-th degree IFE shape functions by enforcing the jump conditions on the interface curve in a weak sense.

The purpose of this article is to report our recent explorations in developing higher degree IFE methods. Specifically, we present a least squares formulation for constructing IFE spaces. This formulation enforces all jump conditions including the chosen extended jump conditions along the actual interface Γ. The existence of a p-th degree IFE shape function is intrinsically guaranteed by the least squares formulation. The uniqueness of the p-th degree IFE shape function is also established under certain conditions. In this framework, the proof for existence and uniqueness does not rely on how elements are cut by the interface, and this feature simplifies the treatment of high-order IFE spaces.

In this article, we discuss p-th degree IFE spaces based on one of the following two groups of extended jump conditions:

- **Normal Extended Jump Conditions**

$$\left[\beta \frac{\partial^j u}{\partial \mathbf{n}^j}\right]_\Gamma = 0,\ j = 2, 3, \dots p, \tag{2}$$

- **Laplacian Extended Jump Conditions**

$$\left[\beta \frac{\partial^j \triangle u}{\partial \mathbf{n}^j}\right]_\Gamma = 0,\ j = 0, 1, 2, \dots p-2. \tag{3}$$

The normal jump conditions for degree $p = 2$ have been discussed in [2, 6] for the straight line interface while in [19], the normal jump conditions are used to construct p-th degree shape functions for curved interface and piecewise constant β. The Laplacian jump conditions (3) have been used in [1, 28].

This manuscript is organized as follows. In Section 2, we outline the notations and assumptions used through the whole manuscript. Then we develop the procedure for constructing local IFE spaces on interface elements. The uniqueness of IFE shape functions is also established under some appropriate conditions. In Section 3, we present numerical experiments for the IFE interpolation and IFE solution to the interface problem. Finally, brief conclusions are given in the last section.

2. p-th Degree IFE Spaces

2.1. Notations and Assumptions. In this article, we only consider triangular meshes of the domain Ω, denoted by $\mathcal{T}_h$. Let $\mathcal{T}_h^i$ and $\mathcal{T}_h^n$ denote the set of all interface elements and non-interface elements in this mesh, respectively. For each element T in $\mathcal{T}_h$, we let $\mathcal{I} = \{1, 2, \dots, \frac{(p+1)(p+2)}{2}\}$ be the set of indices of the usual local nodes $N_i, i \in \mathcal{I}$ associated with the standard p-th degree Lagrange finite element shape functions $\psi_{j,T}$, $j \in \mathcal{I}$ in T, where we recall the following property:

$$\psi_{j,T}(N_i) = \delta_{ij},\ \forall i, j \in \mathcal{I}. \tag{4}$$

We let $\mathbb{P}^p(T)$ be the space of polynomials of degree not exceeding p which is obviously spanned by the finite element shape functions. We also use $\mathcal{N}_h$ to denote the set of local nodes in all elements in a mesh $\mathcal{T}_h$.

Since the standard p-th degree local finite element space will be used over all non-interface elements, we will focus on the development of the local p-th degree IFE spaces on interface elements. Without loss of generality, we assume each interface element $T \in \mathcal{T}_h^i$ is cut by the interface Γ into two subelements $T^1 = \Omega^1 \cap T$ and $T^2 = \Omega^2 \cap T$, by which, we define $\mathcal{I}^1 = \{i : N_i \in T^1\}$ and $\mathcal{I}^2 = \{i : N_i \in T^2\}$ such that $\mathcal{I} = \mathcal{I}^1 \cup \mathcal{I}^2$. Each p-th degree IFE function on T is a macro finite element function chosen from the following piecewise polynomial space:

$$\mathcal{P}^p(T) = \{q : q|_{T^1} \in \mathbb{P}^p(T^1) \text{ and } q|_{T^2} \in \mathbb{P}^p(T^2)\}. \tag{5}$$

Since each function in $\mathcal{P}^p(T)$ is formed by two p-th degree polynomials, we consider the related product polynomial space $\mathcal{S}^p(T) = \left[\mathbb{P}^p(T)\right]^2$, which, by (4), has the following set of basis functions:

$$\xi_{i,T} = \begin{cases} (\psi_{i,T},\, 0), & \text{if } i \in \mathcal{I}^1 \\ (0,\, \psi_{i,T}), & \text{if } i \in \mathcal{I}^2, \end{cases} \qquad \eta_{i,T} = \begin{cases} (0,\, \psi_{i,T}), & \text{if } i \in \mathcal{I}^1 \\ (\psi_{i,T},\, 0), & \text{if } i \in \mathcal{I}^2. \end{cases} \tag{6}$$

We can use the basis functions in (6) to span two subspaces of $\mathcal{S}^p(T)$ as follows:

$$\mathcal{V}_1 = \mathrm{Span}\{\xi_{i,T} : i \in \mathcal{I}\},\ \mathcal{V}_2 = \mathrm{Span}\{\eta_{i,T} : i \in \mathcal{I}\}. \tag{7}$$

It is obvious that the direct sum of the two subspaces in (7) is $\mathcal{S}^p(T)$, i.e.,

$$\mathcal{S}^p(T) = \mathcal{V}_1 \bigoplus \mathcal{V}_2. \tag{8}$$

In fact, the piecewise polynomial space $\mathcal{P}^p(T)$ is isomorphic to the product polynomial space $\mathcal{S}^p(T)$ because of the following one-to-one mapping:

$$\mathcal{F}_T : \mathcal{S}^p(T) \to \mathcal{P}^p(T),\ \mathcal{F}_T v = \begin{cases} v_1, & \text{on } T^1 \\ v_2, & \text{on } T^2, \end{cases} \qquad \forall\ v = (v_1,\, v_2) \in \mathcal{S}^p(T). \tag{9}$$

We can further easily verify that if $\eta \in \mathcal{V}_2$, then

$$\left(\mathcal{F}_T \eta\right)(N_i) = 0,\ \forall\ i \in \mathcal{I}. \tag{10}$$

For any $\widetilde{\Gamma} \subseteq \Gamma$, we introduce a linear operator $[[\cdot]]_{\widetilde{\Gamma}}$ on $\mathcal{S}^p(T)$ which is a generalized form of the jump of a scalar function:

$$[[v]]_{\widetilde{\Gamma}} := v_1|_{\widetilde{\Gamma}} - v_2|_{\widetilde{\Gamma}},\ \forall v = (v_1, v_2) \in \mathcal{S}^p(T), \tag{11}$$

To discuss the construction of the p-th degree IFE spaces, we make the following assumptions about the interface Γ which are similar to those used in [16]:

(H1) The interface Γ cannot intersect an edge of any element at more than two points unless the edge is part of Γ.

(H2) If Γ intersects the boundary of an element at two points, these intersection points must be on different edges of this element.

(H3) The interface Γ is a piecewise C^2 function, and the mesh $\mathcal{T}_h$ is formed such that on every interface element $T \in \mathcal{T}_h^i$, $\Gamma \cap T$ is C^2.

Finally we conclude this section by recalling some notations related to Sobolev spaces and associated norms. For every measurable subset $\tilde{\Omega} \subseteq \Omega$ we let $H^p(\tilde{\Omega})$ be the standard Hilbert space on $\tilde{\Omega}$ equipped with the norm $\|\cdot\|^2_{p,\tilde{\Omega}} = \sum_{|\alpha| \le p} \|D^\alpha v\|^2_{\tilde{\Omega}}$

and semi-norm $|v|^2_{p,\tilde{\Omega}} = \sum_{|\alpha|=p} \|D^\alpha v\|^2_{\tilde{\Omega}}$ where $\|\cdot\|$ is the L^2 norm and α is a multi-index. Furthermore, if $\tilde{\Omega}^k = \tilde{\Omega} \cap \Omega^k \neq \emptyset, \quad k = 1, 2$, we define

$$PH_1^p(\tilde{\Omega}) = \{u : u|_{\tilde{\Omega}^k} \in H^p(\tilde{\Omega}^k),\ k = 1,2;\ [u] = 0,\ [\beta \nabla u \cdot \mathbf{n}_\Gamma] = 0 \text{ on } \Gamma \cap \tilde{\Omega} \text{ and } u \text{ satisfies (2)}\},$$

$$PH_2^p(\tilde{\Omega}) = \{u : u|_{\tilde{\Omega}^k} \in H^p(\tilde{\Omega}^k),\ k = 1,2;\ [u] = 0\ \ [\beta \nabla u \cdot \mathbf{n}_\Gamma] = 0 \text{ on } \Gamma \cap \tilde{\Omega} \text{ and } u \text{ satisfies (3)}\},$$

We equip $PH_1^p(\tilde{\Omega})$ and $PH_2^p(\tilde{\Omega})$ with the broken norms and semi norms

$$\|\cdot\|^2_{p,\tilde{\Omega}} = \|\cdot\|^2_{p,\tilde{\Omega}^1} + \|\cdot\|^2_{p,\tilde{\Omega}^2}, \qquad |\cdot|^2_{p,\tilde{\Omega}} = |\cdot|^2_{p,\tilde{\Omega}^1} + |\cdot|^2_{p,\tilde{\Omega}^2}.$$

2.2. Local IFE Spaces On Interface Elements. Here we provide a general definition of local IFE spaces for each of the extended jump conditions (2) and (3), and then, we construct IFE shape functions using the least squares idea. Existing local IFE spaces in the literature consist of piecewise polynomial functions satisfying the jump conditions exactly for an interface with a simple geometry. For generic curved interfaces (especially non algebraic curves), piecewise polynomial functions are not able to satisfy the interface jump conditions everywhere on the interface. Constructing two p-th degree polynomials together such that they can satisfy jump conditions in a certain sense that can lead to optimally convergent IFE spaces is a major challenge. An attempt to construct p-th degree IFE shape functions on elements cut by nonlinear interfaces was presented in [1] where the interface conditions (including the extended ones) were enforced weakly via a L^2 inner product of suitably chosen polynomials space on the curved interface.

We now extend this weak enforcement idea through a least squares formulation. Note that each p-th degree IFE function ϕ_T on an interface element T should be a macro finite element function chosen from the space $\mathcal{P}^p(T)$ defined in (5) that can satisfy the jump conditions (1c) and (1d) specified in the interface problem (1) and one group of the extended jump conditions (2) or (3). By the isomorphism between the space $\mathcal{P}^p(T)$ and $\mathcal{S}^p(T) = \left[\mathbb{P}^p(T)\right]^2$, a p-th degree IFE function can also be constructed from the product space $\mathcal{S}^p(T)$. Our idea is to define a symmetric positive semi-definite bilinear form on $\mathcal{S}^p(T)$ that is based on a least squares fit of all the jump conditions across the interface, including the chosen extended ones. Then, following the idea used in [2, 3, 6], for each polynomial in $\mathcal{V}_1$, we construct another polynomial from $\mathcal{V}_2$ to minimize the penalty induced from this bilinear form, and the local p-th degree IFE space is formed by piecewise polynomials constructed from polynomials in $\mathcal{V}_1$ and $\mathcal{V}_2$ put together in this least squares framework. In fact, the local p-th degree IFE space to be constructed on T is the orthogonal complement of $\mathcal{V}_2$ with respect to a quasi inner product associated with this bilinear form, and this orthogonality relates the least squares formulation in this article to the weak enforcement idea in [1]. Also, the decomposition of the space $\mathcal{S}^p(T)$ into two subspaces $\mathcal{V}_1$ and $\mathcal{V}_2$ is similar to the idea in [21] where two polynomial spaces are used on interface elements to capture the jump behaviors by enforcing the Nitsche's penalty in the formulation.

Using the extended jumps conditions (2) and (3), we now introduce two bilinear forms on each interface element T. First, we let Γ_T be the extended interface such that $T \cap \Gamma \subseteq \Gamma_T$, as illustrated in Figure 2, and

$$k_1 h < |\Gamma_T| < k_2 h, \quad \forall\, T \in \mathcal{T}_h^i. \tag{12}$$

for some positive constants k_1 and k_2 independent of the mesh size h.

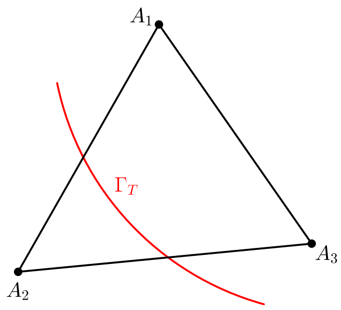

FIGURE 2. An extended local interface Γ_T outside of element T.

Now, for each positive integer p, we consider the following bilinear forms defined on $\mathcal{S}^p(T) \times \mathcal{S}^p(T)$ for the extended jump conditions (2) by

$$\mathcal{J}_1(v, w) = \omega_0 \int_{\Gamma_T} [[v]]_{\Gamma_T}\, [[w]]_{\Gamma_T} ds + \sum_{j=1}^{p} \omega_j \int_{\Gamma_T} \left[\left[\beta \frac{\partial^j v}{\partial \mathbf{n}^j}\right]\right]_{\Gamma_T} \left[\left[\beta \frac{\partial^j w}{\partial \mathbf{n}^j}\right]\right]_{\Gamma_T} ds, \tag{13}$$

and for the extended jump conditions (3) by

$$\begin{aligned} \mathcal{J}_2(v, w) =& \omega_0 \int_{\Gamma_T} [[v]]_{\Gamma_T}\, [[w]]_{\Gamma_T} ds + \int_{\Gamma_T} \omega_1 \left[\left[\beta \frac{\partial v}{\partial \mathbf{n}}\right]\right]_{\Gamma_T} \left[\left[\beta \frac{\partial w}{\partial \mathbf{n}}\right]\right]_{\Gamma_T} ds \\ &+ \sum_{j=0}^{p-2} \omega_{j+2} \int_{\Gamma_T} \left[\left[\beta \frac{\partial^j \triangle v}{\partial \mathbf{n}^j}\right]\right]_{\Gamma_T} \left[\left[\beta \frac{\partial^j \triangle w}{\partial \mathbf{n}^j}\right]\right]_{\Gamma_T} ds, \end{aligned} \tag{14}$$

where $\omega_j > 0$, $j = 0, 1, \ldots, p$ are weights. It is easy to see that these two bilinear forms are symmetric and $\mathcal{J}_k(v, v) \geq 0$ for all $v \in \mathcal{S}^p(T)$, $k = 1, 2$. However, these bilinear forms are positive semi-definite because, if $v = (1, 1) \in \mathcal{S}^p(T)$, we have $\mathcal{J}_1(v, w) = \mathcal{J}_2(v, w) = 0$ for any $w \in \mathcal{S}^p(T)$. Therefore, we can only use these bilinear forms to define semi norms on $\mathcal{S}^p(T)$ as follows:

$$|v|_{\mathcal{J}_k} = \sqrt{\mathcal{J}_k(v, v)},\ k = 1, 2,\ \forall v \in \mathcal{S}^p(T). \tag{15}$$

Now, we consider how to construct an IFE function from a function $v \in \mathcal{S}^p(T)$ whose values at the local Lagrange nodes $N_i, i \in \mathcal{I}$ are known. Hence the construction of an IFE function v is reduced to the requirement that v needs to satisfy the jump conditions (1c) and (1d) and one group of the two possible extended jump conditions in (2) and (3). By their definitions given in (6) and (7), we can see that the subspace $\mathcal{V}_1$ is associated with the nodal values of an IFE function so that the subspace $\mathcal{V}_2$ is somehow related with the jump conditions. Since $\mathcal{J}_k(\cdot, \cdot), k = 1, 2$

is a quasi inner product on $\mathcal{S}^p(T)$, the weak enforcement idea suggests to consider IFE functions from the following spaces:

$$\mathcal{V}_2^{\perp,k} := \{v \in \mathcal{S}^p(T) \,:\, \mathcal{J}_k(v,w) = 0,\ \forall w \in \mathcal{V}_2\}, \qquad k = 1,2, \tag{16}$$

which can be considered as orthogonal complements of $\mathcal{V}_2$ in the sense related to the symmetric positive semi-definite bilinear form $\mathcal{J}_k(\cdot,\cdot), k = 1,2$. In other words, the interface jump conditions are imposed on all functions in $\mathcal{V}_2^{\perp,k}$ weakly through the quasi inner product defined by the bilinear form $\mathcal{J}_k(\cdot,\cdot), k = 1,2$.

By (8), every $v \in \mathcal{V}_2^{\perp,k}$ has a unique representation as

$$v = \xi_T + \eta_T,\ \xi_T \in \mathcal{V}_1, \text{ and } \eta_T \in \mathcal{V}_2. \tag{17}$$

Since we have assumed that $v(N_i) = v_i, i \in \mathcal{I}$ are known, by (6) and (7), we have $\xi_T = \sum_{i\in\mathcal{I}} v_i \xi_{i,T}$ and we need to look for a vector $\mathbf{c} = (c_1, c_2, \dots, c_{|\mathcal{I}|})^T \in \mathbb{R}^{|\mathcal{I}|}$ such that $\eta_T = \sum_{i\in\mathcal{I}} c_i \eta_{i,T}$ leading to

$$v = \sum_{i\in\mathcal{I}} v_i\, \xi_{i,T} + \sum_{i\in\mathcal{I}} c_i\, \eta_{i,T}. \tag{18}$$

Then, to enforce the requirement that $v \in \mathcal{V}_2^{\perp,k}$, we test (18) against $\eta_{i,T},\ i = 1,2,\dots,|\mathcal{I}|$ in $\mathcal{V}_2$ such that $\mathcal{J}_k(v,\eta_{i,T}) = 0$ leading to the linear system

$$\mathbf{A}^{(k)}\mathbf{c} = \mathbf{b}, \tag{19a}$$

where

$$\mathbf{v} = (v_1, v_2, \dots, v_{|\mathcal{I}|})^T,\ \mathbf{b} = -\mathbf{B}^{(k)}\mathbf{v} \in \mathbb{R}^{|\mathcal{I}|\times 1}, \tag{19b}$$

and

$$\mathbf{A}^{(k)} = \left(\mathcal{J}_k(\eta_{i,T}, \eta_{j,T})\right)_{i,j\in\mathcal{I}} \in \mathbb{R}^{|\mathcal{I}|\times|\mathcal{I}|}, \tag{19c}$$

$$\mathbf{B}^{(k)} = \left(\mathcal{J}_k(\xi_{i,T}, \eta_{j,T})\right)_{i,j\in\mathcal{I}} \in \mathbb{R}^{|\mathcal{I}|\times|\mathcal{I}|}. \tag{19d}$$

We now discuss the existence for such a vector $\mathbf{c}$ that satisfies (19a) which leads to an IFE function $\mathcal{F}_T v \in \mathcal{P}^p(T)$ with v defined by (18). This existence is not obvious because the positive semi-definiteness of the bilinear form $\mathcal{J}_k(\cdot,\cdot), k = 1,2$ can only guarantee the positive semi-definiteness of the matrix $\mathbf{A}^{(k)}$. However, even though it is unclear whether $\mathbf{A}^{(k)}$ is always invertible, we show that the linear system (19a) always has a solution as stated in the following theorem.

Theorem 2.1 (Existence)**.** *On every interface element $T \in \mathcal{T}_h^i$, $\mathbf{b} = -\mathbf{B}^{(k)}\mathbf{v}$ is in $\mathrm{Ran}(\mathbf{A}^{(k)}), k = 1,2$ for each vector $\mathbf{v} \in \mathbb{R}^{|\mathcal{I}|}$.*

Proof. Essentially, we only need to show that $\mathrm{Ran}(\mathbf{B}^{(k)}) \subseteq \mathrm{Ran}(\mathbf{A}^{(k)})$, which is equivalent to $\mathrm{Ker}(\mathbf{A}^{(k)}) \subseteq \mathrm{Ker}\left((\mathbf{B}^{(k)})^T\right)$. By contradiction, assume that there exists some $\hat{\mathbf{c}} = (\hat{c}_i)_{i\in\mathcal{I}} \in \mathbb{R}^{|\mathcal{I}|}$ such that $\mathbf{A}^{(k)}\hat{\mathbf{c}} = 0$ but $(\mathbf{B}^{(k)})^T\hat{\mathbf{c}} \neq 0$, then we can find a vector $\hat{\mathbf{d}} = (\hat{d})_{i\in\mathcal{I}} \in \mathbb{R}^{|\mathcal{I}|}$ such that $\hat{\mathbf{d}}^T \left(\mathbf{B}^{(k)}\right)^T \hat{\mathbf{c}} > 0$.

Letting $\hat{\mathbf{v}} = \epsilon\hat{\mathbf{d}}$ with $\epsilon < 0$ and letting $\hat{\zeta}_T = \sum_{i\in\mathcal{I}} \hat{v}_i\, \xi_{i,T} + \sum_{i\in\mathcal{I}} \hat{d}_i\, \eta_{i,T}$, we have

$$\begin{aligned}\mathcal{J}_k(\hat{\zeta}_T,\, \hat{\zeta}_T) &= \hat{\mathbf{c}}^T\mathbf{A}^{(k)}\hat{\mathbf{c}} + 2\hat{\mathbf{c}}^T\mathbf{B}^{(k)}\hat{\mathbf{v}} + \hat{\mathbf{v}}^T\mathbf{C}^{(k)}\hat{\mathbf{v}} \\ &= 2\epsilon\hat{\mathbf{c}}^T\mathbf{B}^{(k)}\hat{\mathbf{d}} + \epsilon^2\hat{\mathbf{d}}^T\mathbf{C}^{(k)}\hat{\mathbf{d}}\end{aligned}$$

in which

$$\mathbf{C}^{(k)} = \mathcal{J}_k(\xi_{i,T},\, \xi_{j,T})_{i,j\in\mathcal{I}} \in \mathbb{R}^{|\mathcal{I}|\times|\mathcal{I}|}.$$

Since $\mathbf{C}^{(k)}$ is a symmetric positive semi-definite matrix, we have $\hat{\mathbf{c}}^T\mathbf{C}^{(k)}\hat{\mathbf{c}} \geqslant 0$. For $\epsilon < 0$ small enough we have $\mathcal{J}_k(\hat{\zeta}_T, \hat{\zeta}_T) < 0$ which contradicts the positive semi-definiteness of $\mathcal{J}_k$. This completes the proof. $\square$

Note that the semi norm $|\cdot|_{\mathcal{J}_k}, k = 1, 2$ in (15) actually measures how well the jump conditions are satisfied. Hence, it is important for us to note that the above construction procedure for an IFE function can be considered from the point of view of a least squares fitting as follows:

$$\min_{\eta_T\in\mathcal{V}_2} |v|^2_{\mathcal{J}_k} = \min_{\eta_T\in\mathcal{V}_2} |\xi_T + \eta_T|^2_{\mathcal{J}_k}\,,\ k = 1, 2, \tag{20}$$

where v is given in the form of (18) with known coefficients $\mathbf{v} = (v_1, v_2, \ldots, v_{|\mathcal{I}|})^T$. By the definition of the bilinear form $\mathcal{J}_k(\cdot, \cdot), k = 1, 2$, we can see that this least squares problem is equivalent to finding a minimizer of the following function

$$J_k(\mathbf{c}) = |\zeta_T|^2_{\mathcal{J}_k} = \mathbf{c}^T\mathbf{A}^{(k)}\mathbf{c} + 2\mathbf{c}^T\mathbf{B}^{(k)}\mathbf{v} + \mathbf{v}^T\mathbf{C}^{(k)}\mathbf{v} \geqslant 0. \tag{21}$$

By standard arguments, we know that the minimizer of $J_k(\mathbf{c})$ must satisfy

$$\nabla J_k(\mathbf{c}) = 2\mathbf{A}^{(k)}\mathbf{c} + 2\mathbf{B}^{(k)}\mathbf{v} = 2\left(\mathbf{A}^{(k)}\mathbf{c} + \mathbf{b}\right) = 0,$$

which is equivalent to the linear system (19a).

In a nutshell, given a vector $\mathbf{v} = (v_1, v_2, \ldots, v_{|\mathcal{I}|})^T$, by Theorem 2.1, we can always solve the linear system (19a) to obtain a vector $\mathbf{c} = (c_1, c_2, \ldots, c_{|\mathcal{I}|})^T$. These two vectors lead to a function $v \in \mathcal{V}_2^{\perp,k} \subseteq \mathcal{S}^p(T)$ in the form given in (18) which further yields a function $\phi_T \in \mathcal{P}^p(T)$ by the isomorphic mapping $\mathcal{F}_T$ as follows:

$$\phi_T = \mathcal{F}_T v = \begin{cases} \phi_T^1 = \sum_{i\in\mathcal{I}^1} v_i\,\psi_{i,T} + \sum_{i\in\mathcal{I}^2} c_i\,\psi_{i,T}, \text{ on } T^1 \\ \phi_T^2 = \sum_{i\in\mathcal{I}^2} v_i\,\psi_{i,T} + \sum_{i\in\mathcal{I}^1} c_i\,\psi_{i,T}, \text{ on } T^2. \end{cases} \tag{22}$$

The function ϕ_T constructed above is a p-th degree IFE function on the interface element T because, according to the discussion above, ϕ_T can satisfy the jump conditions of the interface problem on the actual interface Γ in a least squares sense, including the extended ones specified by either (2) or (3).

Now, we describe the construction the local p-th degree IFE space on an interface element T. First, we construct $|\mathcal{I}|$ p-th degree IFE shape functions as follows: Choose a basis $\{\mathbf{v}_i\}_{i=1}^{|\mathcal{I}|}$ in $\mathbb{R}^{|\mathcal{I}|}$,

then, for $i = 1, 2, \ldots, |\mathcal{I}|$, do
step 1: Set $\mathbf{b}_i = -\mathbf{B}^{(k)}\mathbf{v}_i$ and then solve $\mathbf{A}^{(k)}\mathbf{c}_i = \mathbf{b}_i$ for $\mathbf{c}_i = (c_{1,i}, c_{2,i}, \ldots, c_{|\mathcal{I}|,i})$.
step 2: Use $\mathbf{v}_i$ and $\mathbf{c}_i$ in (22) to form the IFE shape function $\phi_{i,T}$.

Then, we define the local p-th degree IFE space on an interface element T as

$$S^p_{k,h}(T) = \text{Span}\{\phi_{i,T},\ i = 1, 2, \ldots, |\mathcal{I}|\},\ k = 1, 2. \tag{23}$$

By the facts that $\text{Dim}(\mathcal{V}_2) = |\mathcal{I}|$ and the positive semi-definiteness of $\mathcal{J}_k$, we know $\text{Dim}(\mathcal{V}_2^{\perp,k}) \geq |\mathcal{I}|$. Then, because $\mathcal{F}_T$ is an isomorphism, we know that $\text{Dim}(\mathcal{F}_T\mathcal{V}_2^{\perp,k}) \geq |\mathcal{I}|$. Therefore, in general, the local IFE space $S^p_{k,h}(T)$ defined in (23) is just one of subspaces of $\mathcal{F}_T\mathcal{V}_2^{\perp,k}$. Different ways to choose $\{\mathbf{v}_i\}_{i=1}^{|\mathcal{I}|}$ and different ways to generate a vector $\mathbf{c}_i$ from $\mathbf{A}^{(k)}\mathbf{c}_i = \mathbf{b}_i$ may yield different local IFE spaces on an interface element T. Even for a fixed set of vectors $\{\mathbf{v}_i\}_{i=1}^{|\mathcal{I}|}$, the indefiniteness of the linear system $\mathbf{A}^{(k)}\mathbf{c}_i = \mathbf{b}_i$ can still lead to different local IFE spaces unless $\mathbf{A}^{(k)}$ is nonsingular which will be addressed in the next subsection. On the other hand, the procedure presented above allows us to choose a set of linearly independent vectors $\{\mathbf{v}_i\}_{i=1}^{|\mathcal{I}|}$ for generating a local IFE space $S_{k,h}^p(T)$ of our preference. For example, if we let $\mathbf{v}_i = \mathbf{e}_i, 1 \le i \le |\mathcal{I}|$, then the procedure above leads to the following Lagrange type IFE shape functions:

$$(24)\quad \phi_{i,T} = \psi_{i,T} + \psi_{i,T}^{(0)},\ \psi_{i,T}^{(0)} = \begin{cases} \sum_{j\in\mathcal{I}^2} c_{j,i}\,\psi_{j,T}, & \text{on } T^1 \\ \sum_{j\in\mathcal{I}^1} c_{j,i}\,\psi_{i,T}, & \text{on } T^2, \end{cases} \qquad i = 1, 2, \dots, |\mathcal{I}|.$$

For illustration, we present plots for all the 6 quadratic Lagrange type IFE shape functions on a typical interface element in Figure 3. We also note that, even though each IFE shape function is constructed to satisfy the jump conditions in a least squares sense, we have observed that its components on subelements match each other at p points or more on the interface Γ. A similar phenomenon was also observed by Adjerid et al. [1]. We illustrate this phenomenon by plots in Figures 4-7 for the jump $\phi_{1,T}^1 - \phi_{1,T}^2$ along the curve Γ_T on a typical interface element, from which we can see that, under both extended jump conditions, the quadratic IFE shape function is continuous at 2 points on Γ_T while the cubic IFE shape function is continuous at 3 points on Γ_T.

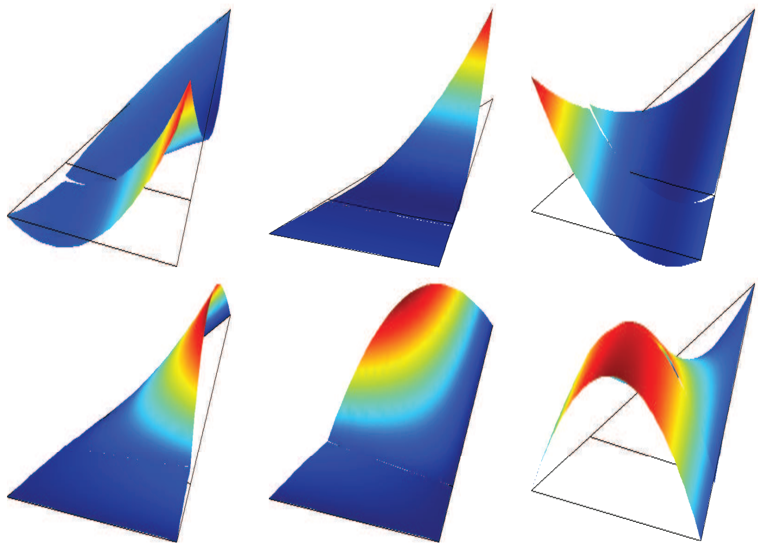

FIGURE 3. Plots in the first row are quadratic IFE shape functions associated with the vertices of the interface element, those in the second row are quadratic IFE shape functions associated with the edges.

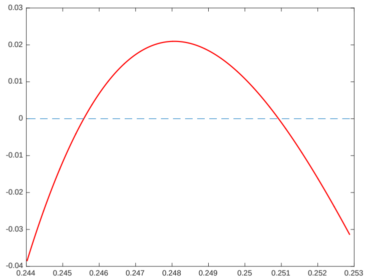

FIGURE 4. The jump $\phi^1_{1,T} - \phi^2_{1,T}$ versus t for $p = 2$ and the normal jump conditions.

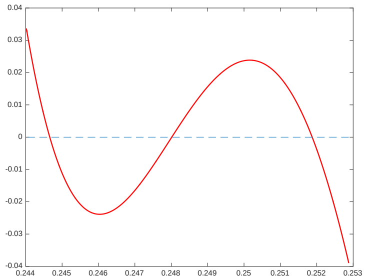

FIGURE 5. The jump $\phi^1_{1,T} - \phi^2_{1,T}$ versus t for $p = 3$ and the normal jump conditions.

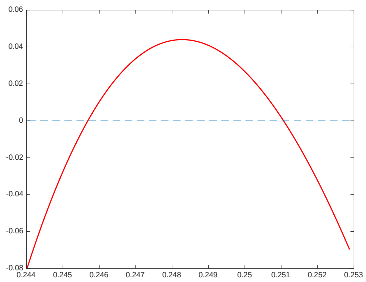

FIGURE 6. The jump $\phi^1_{1,T} - \phi^2_{1,T}$ versus t for $p = 2$ and Laplacian jump conditions.

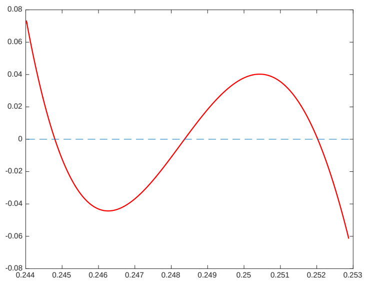

FIGURE 7. The jump $\phi^1_{1,T} - \phi^2_{1,T}$ versus t for $p = 3$ and Laplacian jump conditions.

To end this section, we note that extending the local interface $T \cap \Gamma$ to Γ_T outside an interface element T, as illustrated in Figure (12), is inspired by the idea in [18] where Guzman *et al.* used it to establish error estimates. Through numerical experiments, we have noticed that this extension technique is useful for improving the conditioning of the linear system in (19a). Specifically, if the bilinear forms are defined on the interface $\Gamma \cap T$ instead of its extension Γ_T, the linear system (19a) might become too ill-conditioned to be solved accurately when one of the sub-elements T^1 and T^2 is extremely small or $\Gamma \cap T$ is very short. We now present an numerical example to show the dependence of the condition number of the matrix in (19a) on the relative location of the interface as well as the ratio of β^1 and β^2 and to demonstrate that using bilinear forms defined on an extended interface can improve the condition of this matrix.

To be specific, we consider the domain $\Omega = (-1,1)\times(-1,1)$ and a sequence of interfaces that are circles $x^2+y^2 = \pi/6.28 - 0.25r$ with shrinking radii for $r = 0,1,2,4,5$. The interface elements studied have the vertices: $(-0.6,0)$, $(-0.4,0)$, $(-0.6,0.2)$ in which the 5 locations of the interfaces corresponding to $r = 0,1,2,4,5$ are shown in Figure 8. In this interface element, we denote the left sub-element by T^1 and the right one by T^2, we let $\beta^1 = 1$ and let the value of β^2 be either 5 or 100. Table 1 presents the condition number of the matrix in (19a) for constructing the IFE shape function associated with the vertex $(-0.6,0)$ using the normal extended jump conditions in the bilinear forms defined only on $T\cap\Gamma$ instead of its extension. We note that the condition number of this matrix becomes larger as either the degree p or the ratio β^2/β^1 increases, and this matrix becomes extremely ill-conditioned when the interface is at the 5-th location due to the fact that T^2 or $\Gamma\cap T$ is too small. When bilinear form is defined on the extended interface Γ_T such that $|\Gamma_T - (\Gamma\cap T)| = 0.3h$, the condition number of this matrix is improved as demonstrated by the data in Table 2, especially for the difficult cases when the interface is at the 4-th and 5-th locations. Developing methods to improve the conditioning for the linear system (19a) in such extreme cases is an interesting research topic in the future.

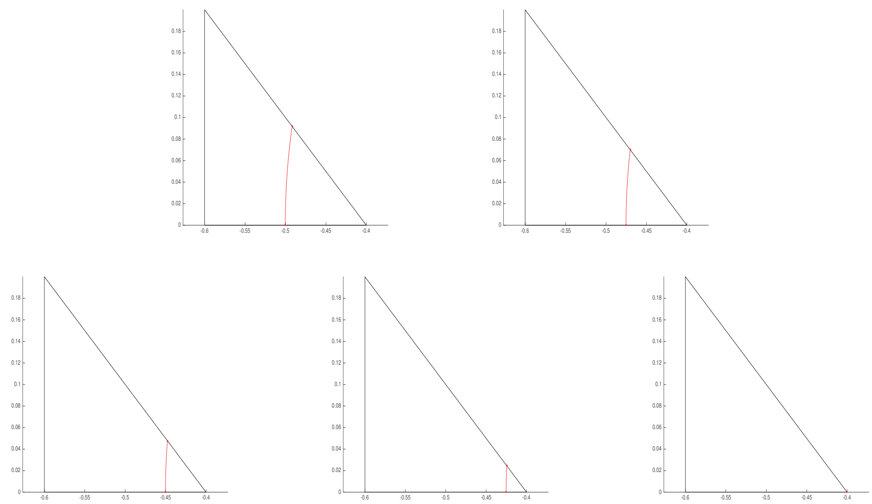

FIGURE 8. An interface element in which the interface is at different locations.

TABLE 1. Without Extension.

Interface Locations	$\beta^2=5,\ p=2$	$\beta^2=5,\ p=3$	$\beta^2=100,\ p=2$	$\beta^2=100,\ p=3$
Location 1	7.1557E+3	4.3476E+6	1.3312E+6	5.9246E+8
Location 2	6.4376E+3	1.3027E+7	1.4657E+6	1.9756E+9
Location 3	4.3064E+4	1.3765E+7	1.1231E+7	2.2153E+9
Location 4	1.0591E+6	9.0351E+8	2.8705E+8	2.3425E+11
Location 5	2.3013E+14	1.7583E+21	6.2169E+16	3.6076E+21

TABLE 2. With Extension.

Interface Locations	$\beta^2 = 5,\ p = 2$	$\beta^2 = 5,\ p = 3$	$\beta^2 = 100,\ p = 2$	$\beta^2 = 100,\ p = 3$
Location 1	1.7675E+3	6.9292E+4	2.8910E+5	1.2266E+7
Location 2	1.6010E+3	1.4341E+5	2.5362E+5	2.1539E+7
Location 3	7.8285E+3	2.5890E+5	1.4721E+6	4.0909E+7
Location 4	8.7303E+4	7.7764E+6	2.4242E+7	1.8945E+9
Location 5	8.9091E+9	6.8934E+16	3.0013E+10	8.4763E+16

2.3. Unique Determination of IFE Functions. We now discuss whether a p-th degree IFE function in an interface element T can be uniquely determined by its values at the local nodes $N_i \in T, i = 1, 2, \ldots, |\mathcal{I}|$. We will focus on the case in which the curvature of $T \cap \Gamma$ is not the zero function and we refer readers to [2, 6] for related discussions about the case in which $T \cap \Gamma$ is a line. Since the unique determination of a p-th degree IFE function is equivalent to the definiteness of $\mathbf{A}^{(k)}$ which is decided by the definiteness of $\mathcal{J}_k$, we investigate the following set which can be considered as the kernel of $\mathcal{J}_k$:

$$\mathcal{K}_k := \text{Ker } (\mathcal{J}_k) = \{v \in \mathcal{S}^p(T) \, : \, \mathcal{J}_k(v, w) = 0, \ \forall w \in \mathcal{S}^p(T)\}, \ k = 1, 2. \tag{25}$$

Since $\mathcal{S}^p(T)$ consists of piecewise polynomials, we know that the elements of $\mathcal{K}_k$ satisfy the physical and extended jump conditions exactly; hence, we can express $\mathcal{K}_k$ as

$$\mathcal{K}_k = \{v \in \mathcal{S}^p(T) \, : \, |v|_{\mathcal{J}_k} = 0\}, \ k = 1, 2. \tag{26}$$

Let us first consider the case that involves the normal extended jump conditions (2).

Lemma 2.1. *Assume T is an interface element such that $\Gamma \cap T$ has a nonzero curvature. Then*

$$\mathcal{K}_1 \subseteq \{v = (v_1, v_2) \in \mathcal{S}^p(T) \, : \, \nabla(\beta_1 v_1 - \beta_2 v_2) = \mathbf{0}\}. \tag{27}$$

Proof. Let $v = (v_1, v_2)$ be an arbitrary element of $\mathcal{K}_1$ and X be an arbitrary point in $T \cap \Gamma$ where the normal of $T \cap \Gamma$ is $\mathbf{n}$. Consider the p-th degree function $g_{\mathbf{n}}(t) = \beta_1 v_1(X + \mathbf{n}t) - \beta_2 v_2(X + \mathbf{n}t)$. Then, by (26), we have

$$\frac{d^j g_{\mathbf{n}}}{dt^j}(0) = \left[\beta \frac{\partial^j v}{\partial \mathbf{n}^j}(X)\right] = 0, \ j = 1, 2, \ldots, p.$$

Hence, $g_{\mathbf{n}}$ is a constant which implies that the polynomial function $\beta_1 v_1 - \beta_2 v_2$ is a constant on each line normal to $\Gamma \cap T$.

Let $(\tilde{x}, \tilde{y})$ be a local coordinate system around T as shown in Figure (9) and assume we can describe $\Gamma \cap T$ by $\tilde{y} = s(\tilde{x})$. Because $\Gamma \cap T$ is assumed to be a C^2 curve with a non zero curvature, there exists a point $Y_0 = (\tilde{x}_0, \tilde{y}_0) \in \Gamma \cap T$ such that $s''(\tilde{x}_0) > 0$, and, by the continuity of s'', there exists a ball $B_\epsilon(Y_0) := \{X \, : \, |X - Y_0| \leqslant \epsilon\}$, for some $\epsilon > 0$ such that $s''(\tilde{x}) > 0$ for all $(\tilde{x}, \tilde{y}) \in B_\epsilon(Y_0) \cap \Gamma$. Hence, s' is strictly increasing on $B_\epsilon(Y_0) \cap \Gamma$. Now, let $Y_1 \in B_\epsilon(Y_0) \cap \Gamma$ be arbitrary but $Y_1 \neq Y_0$ and let l_0 and l_1 be the lines at Y_0 and Y_1 normal to Γ, respectively. By the result shown above, there exist two constants $C_k, k = 0, 1$ such that $\beta_1 v_1(X) - \beta_2 v_2(X) = C_k \ \forall X \in l_k, \ k = 0, 1$. Since s' is a strictly increasing function on $B_\epsilon(Y_0) \cap \Gamma$, the normal lines l_0 and l_1 have distinct slopes and they must intersect as illustrated in Figure 10, which implies $C_0 = C_1$. Since Y_1 is an arbitrary point on $B_\epsilon(Y_0) \cap \Gamma$, we conclude that $(\beta_1 v_1 - \beta_2 v_2)|_{B_\epsilon(Y_0)} \equiv C_0$ and this further implies that $\beta_1 v_1 - \beta_2 v_2$ is a constant polynomial. Then, we must have $\nabla(\beta_1 v_1 - \beta_2 v_2) = \mathbf{0}$ for every $v = (v_1, v_2) \in \mathcal{K}_1$; hence, (27) is proven. $\square$

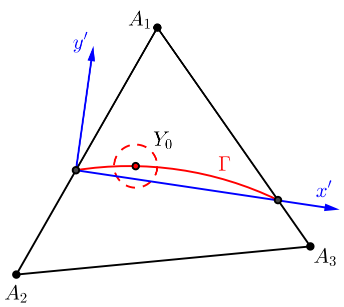

FIGURE 9. The local system.

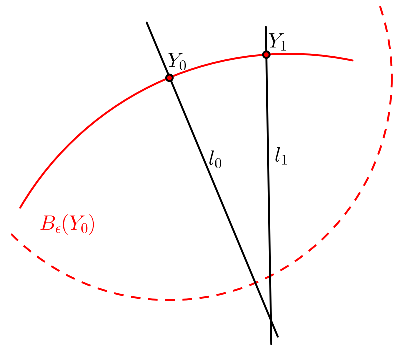

FIGURE 10. Any two normal lines intersect.

Now we are ready to prove that $\mathcal{J}_1$ is positive definite as stated in the next lemma.

Lemma 2.2. *Let T be an interface element such that $\Gamma \cap T$ has a non zero curvature, then the bilinear form $\mathcal{J}_1$ is positive definite on the subspace $\mathcal{V}_2$.*

Proof. First, we show that $\mathcal{V}_2 \cap \mathcal{K}_1 = \{(0,0)\}$. Consider an arbitrary $v = (v_1, v_2) \in \mathcal{V}_2 \cap \mathcal{K}_1$. Let e be an interface edge of T that intersects Γ at D and, without loss of generality, assume the first $p+1$ nodes N_i, $i = 1, 2, \ldots, p+1$ of T are on e as illustrated in Figure (11).

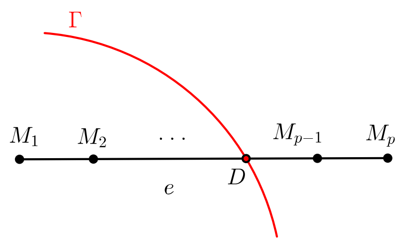

FIGURE 11. The interface edge.

Because $v = (v_1, v_2) \in \mathcal{V}_2 \cap \mathcal{K}_1$, we have $|v|_{\mathcal{J}_1} = 0$. Thus v satisfies the jump conditions everywhere so that $v_1(D) = v_2(D)$. By Lemma 2.1, we also have $\beta_1 \nabla v_1 - \beta_2 \nabla v_2 = 0$ which leads to

$$\beta_1 \frac{\partial^j v_1}{\partial \mathbf{t}_e^j} = \beta_2 \frac{\partial^j v_2}{\partial \mathbf{t}_e^j}, \quad j = 1, 2, \ldots, p, \tag{28}$$

where $\mathbf{t}_e$ is a unit vector parallel to the edge e. Hence, by the continuity at D and (28), $v_1|_e$ and $v_2|_e$ are two functions on e that satisfy the 1-D elliptic jump conditions specified in [3]. Moreover, by (10), $v \in \mathcal{V}_2$ means to $v_1(M_i) = 0$ for $M_i \in T^1$ and $v_2(M_i) = 0$ for $M_i \in T^2$. Thus, by Theorem 2.1 in [3] for the uniqueness of 1-D IFE shape functions, we have $v_1 \equiv v_2 \equiv 0$ on e; therefore, $\beta_1 v_1 - \beta_2 v_2 \equiv 0$ on e. From Lemma 2.1 $\beta_1 v_1 - \beta_2 v_2$ is a constant, we have $\beta_1 v_1(X) - \beta_2 v_2(X) \equiv 0$ for all $X = (x, y)$. So $v_1(N_i) = \frac{\beta_2}{\beta_1} v_2(N_i) = 0$ for $i \in \mathcal{I}^2$ which means that $v_1(N_i) = 0$ for all $i \in \mathcal{I}$, and so that $v_1 \equiv 0$. Similarly, we have $v_2 \equiv 0$. Hence, $v = (0, 0)$ implying $\mathcal{K}_1$ only contains trivial functions in $\mathcal{V}_2$.

Finally, let $v = (v_1, v_2) \in \mathcal{V}_2$ be such that $\mathcal{J}_1(v, v) = 0$. Then v is in $\mathcal{V}_2 \cap \mathcal{K}_1$; hence, $v = (0, 0)$ so that $\mathcal{J}_1$ must be positive definite on $\mathcal{V}_2$. □

Lemma 2.2 leads to the following theorem about unique determination of an IFE function satisfying the normal extended jump conditions (2).

Theorem 2.2 (Uniqueness). *Let T be an interface element such that $\Gamma \cap T$ has a non zero curvature, then $\mathbf{A}^{(1)}$ is nonsingular and every p-th degree IFE function satisfying the normal extended jump conditions is uniquely determined by its values at the nodes in T.*

Proof. Lemma 2.2 implies that the bilinear form $\mathcal{J}_1$ is an inner product on the subspace $\mathcal{V}_2$. Thus, by (19c), the matrix $\mathbf{A}^{(1)}$ is symmetric positive definite from which all results in this theorem follow. □

For the Laplacian extended jump conditions, it is unclear to the authors how to prove the uniqueness of the p-th degree IFE shape functions in the general case. But, we can prove the uniqueness in the cases when the interface $\Gamma \cap T$ is a non-algebraic curve or algebraic curve of degree not less than $p + 1$.

Theorem 2.3 (Uniqueness). *Let T be an interface element such that $\Gamma \cap T$ is not an algebraic curve or an algebraic curve of degree at least $p + 1$. Then $\mathbf{A}^{(2)}$ is nonsingular and every p-th degree IFE function satisfying the Laplacian extended jump conditions is uniquely determined by its values at the nodes in T.*

Proof. If $v = (v_1, v_2) \in \mathcal{V}_2 \cap \mathcal{K}_2$, then $q = v_1 - v_2$ is zero on $\Gamma \cap T$. Since it is a polynomial of degree p and Γ is a non-algebraic curve or algebraic curve of degree at least $p + 1$, then $q = 0$ and $v_1(x, y) = v_2(x, y)$ for all x, y by the definition of the algebraic curve in [15]. Then, because $v = (v_1, v_2) \in \mathcal{V}_2$, we have $v = \mathbf{0}$ and $\mathcal{J}_2$ is non-degenerate on $\mathcal{V}_2$. Hence $A^{(2)}$ is a nonsingular matrix and other results follow. □

Under the assumptions of Theorems 2.2 and 2.3, the bilinear forms $\mathcal{J}_k$, $k = 1, 2$ are positive definite on $\mathcal{V}_2$, and we can show that the local IFE space $S^p_{k,h}(T)$ is exactly the space $\mathcal{F}_T \mathcal{V}_2^{\perp,k}$ by the following theorem.

Theorem 2.4. *Let T be an interface element and let $S^p_{k,h}(T)$ be the p-th degree IFE space defined by either the normal or Laplacian jump conditions, and assume, correspondingly, that T satisfies the conditions of either Theorem 2.2 or Theorem 2.3. Then $S^p_{k,h}(T) = \mathcal{F}_T \mathcal{V}_2^{\perp,k}$.*

Proof. Since $\mathcal{J}_k$, $k = 1, 2$, are non-degenerate on the subspace $\mathcal{V}_2$, according to [38], we have $\mathcal{S}^p(T) = \mathcal{V}_2 \oplus \mathcal{V}_2^{\perp,k}$. Note that $\mathrm{Dim}(\mathcal{V}_2) = |\mathcal{I}|$ and $\mathrm{Dim}(\mathcal{S}^p(T)) = 2|\mathcal{I}|$.

By the isomorphism $\mathcal{F}_T$, $\mathrm{Dim}(\mathcal{V}_2^{\perp,k}) = \mathrm{Dim}(\mathcal{F}_T\mathcal{V}_2^{\perp,k}) = |\mathcal{I}|$. Since $S^p_{k,h}(T)$ is the subspace of $\mathcal{F}_T\mathcal{V}_2^{\perp,k}$ with the dimension $|\mathcal{I}|$, we must have $S^p_{k,h}(T) = \mathcal{F}_T\mathcal{V}_2^{\perp,k}$. □

By the uniqueness result we state and prove that the IFE shape functions form a partition of unity. To be specific, let $\phi_{i,T},\ i \in \mathcal{I}$ be the p-th degree IFE shape functions on an interface element T constructed according to the jump conditions in (1) plus either the normal extended jump condition (2) or the Laplacian extended jump conditions (3).

Theorem 2.5 (Partition of Unity). *Let T be an interface interface and assume that it satisfies the conditions in either Theorem 2.2 or Theorem 2.3. Then, p-th degree IFE shape functions constructed with the corresponding extended jump conditions have the following partition of unity property:*

$$\sum_{i\in\mathcal{I}} \phi_{i,T} \equiv 1. \tag{29}$$

Proof. Let $\phi_T = \sum_{i\in\mathcal{I}} \phi_{i,T}$. Then ϕ_T is an IFE function and $\phi_T(N_i) = 1$ for $i \in \mathcal{I}$. Thus, there exists a vector $\mathbf{c} = (c_1, c_2, \dots, c_{|\mathcal{I}|})$ solving (19a) such that

$$\zeta_T = \mathcal{F}_T^{-1}\phi_T = \sum_{i\in\mathcal{I}} \xi_{i,T} + \sum_{i\in\mathcal{I}} c_i\eta_{i,T} \in \mathcal{V}_2^{\perp,k}.$$

On the other hand, consider the following function of $\mathcal{S}^p(T)$:

$$\zeta_T^0 = \sum_{i\in\mathcal{I}} \xi_{i,T} + \sum_{i\in\mathcal{I}} \eta_{i,T}.$$

By the partition of unity of the standard finite element shape functions $\psi_{i,T}, 1 \le i \le |\mathcal{I}|$, we have

$$\zeta_T^0 = \big(\sum_{i\in\mathcal{I}} \psi_{i,T}, \sum_{i\in\mathcal{I}} \psi_{i,T}\big) = (1,1)$$

which further implies that $\zeta_T^0 \in \mathcal{V}_2^{\perp,k}$. By Theorem 2.2 or Theorem 2.3, we know that $\zeta_T = \zeta_T^0$. Thus

$$\sum_{i\in\mathcal{I}} \phi_{i,T} = \phi_T = \mathcal{F}_T(\zeta_T) = \mathcal{F}_T(\zeta_T^0) = \begin{cases} 1, & \text{on } T^1, \\ 1, & \text{on } T^2, \end{cases}$$

which proves the partition of unity stated in (29). □

3. Numerical Examples

In this section, we numerically demonstrate that the p-th degree IFE spaces constructed by the least squares method can perform optimally as well as some additional features. For this purpose, we will consider the IFE interpolation and IFE solution in the following p-th degree IFE spaces defined on the solution domain Ω of the interface problem described by (1):

(30)
$$\begin{aligned} S^p_{k,h}(\Omega) = \Big\{ & v \in L^2(\Omega)\ :\ v|_T \in S^p_{k,h}(T)\ \forall T \in \mathcal{T}_h \text{ and} \\ & v|_{T_1}(X) = v|_{T_2}(X)\ \forall T_1, T_2 \in \mathcal{T}_h \text{ such that } X \in (T_1 \cap T_2) \cap \mathcal{N}_h \Big\}, \end{aligned} \quad k = 1, 2$$

where

$$S_{k,h}^p(T) = \begin{cases} \mathrm{Span}\{\phi_{i,T},\ i = 1, 2, \ldots, |\mathcal{I}|\}, & \text{for } T \in \mathcal{T}_h^i, \\ \mathrm{Span}\{\psi_{i,T},\ i = 1, 2, \ldots, |\mathcal{I}|\}, & \text{for } T \in \mathcal{T}_h^n, \end{cases} \quad k = 1, 2,$$

and $\phi_{i,T},\ i = 1, 2, \ldots, |\mathcal{I}|$ are the Lagrange type IFE shape functions defined by (24).

For a function $u \in C^0(\overline{\Omega})$, we define its local p-th degree IFE interpolation on each element $T \in \mathcal{T}_h$ to be the function $I_{h,T}u \in S_{k,h}^p(T)$ such that

$$I_{h,T}u = \begin{cases} \sum_{i\in\mathcal{I}} u(N_i)\psi_{i,T}, & \text{if } T \in \mathcal{T}_h^n, \\ \sum_{i\in\mathcal{I}} u(N_i)\phi_{i,T}, & \text{if } T \in \mathcal{T}_h^i. \end{cases} \tag{31}$$

Then, we define the p-th degree IFE interpolation of u as a function $I_h u \in S_{k,h}^p(\Omega)$ piecewisely by

$$(I_h u)|_T = I_{h,T}u, \quad \forall\, T \in \mathcal{T}_h. \tag{32}$$

For the interface problem (1), we will consider its p-th degree IFE solution generated by applying the p-th degree IFE space in (30) to the partially penalized method discussed in [25, 36]. Specifically, the IFE solution u_h is a function in $S_{k,h}^p(\Omega)$ such that

$$a_h(u_h, v_h) = \int_\Omega f v_h dX,\ \forall v_h \in S_{k,h,0}^p(\Omega), \tag{33}$$

and $u_h(X) = g(X)\ \forall X \in \partial\Omega \cap \mathcal{N}_h$, where the bilinear form a_h is

$$\begin{aligned} a_h(u_h, v_h) = &\sum_{T\in\mathcal{T}_h} \int_T \beta\nabla u_h \cdot \nabla v_h dX + \sum_{e\in\mathring{\mathcal{E}}_h^i} \int_e \{\beta\nabla u_h \cdot \mathbf{n}_e\}_e [v_h]_e ds \\ &+ \epsilon \sum_{e\in\mathring{\mathcal{E}}_h^i} \int_e \{\beta\nabla v_h \cdot \mathbf{n}_e\}_e [u_h]_e ds + \sum_{e\in\mathring{\mathcal{E}}_h^i} \frac{\sigma_e^0}{|e|} \int_e [u_h]_e\, [v_h]_e ds \\ &- \sum_{e\in\mathcal{E}_h^i\cap\partial\Omega} \int_e \beta\nabla u_h \cdot \mathbf{n}_e v_h ds, \end{aligned} \tag{34}$$

in which, $\mathcal{E}_h^i$ and $\mathring{\mathcal{E}}_h^i$ are the set of all interface edges and the set of interior interface edges, respectively, $\{\cdot\}_e$ and $[\cdot]_e$ are the usual average and jump at an edge e. Here $\epsilon = -1, 0, 1$ corresponds to symmetric, incomplete and nonsymmetric partially penalized IFE methods. For more details about this formulation, we refer the readers to [36].

Table 3. Interpolation errors and convergence rates for quadratic IFE spaces, $\beta_1 = 1$ and $\beta_2 = 5$.

	Normal extended jump conditions				Laplacian extended jump conditions			
h	$\|u - I_h u\|_{0,\Omega}$	rate	$\|u - I_h u\|_{1,\Omega}$	rate	$\|u - I_h u\|_{0,\Omega}$	rate	$\|u - I_h u\|_{1,\Omega}$	rate
1/10	2.2372E-3	NA	7.8443E-2	NA	2.2129E-3	NA	7.7412E-2	NA
1/20	2.8229E-4	2.9864	1.9706E-2	1.9930	2.8221E-4	2.9711	1.9712E-2	1.9735
1/40	3.5504E-5	2.9912	4.9525E-3	1.9924	3.5451E-5	2.9929	4.9456E-3	1.9949
1/80	4.4515E-6	2.9956	1.2413E-3	1.9963	4.4466E-6	2.9950	1.2399E-3	1.9959
1/160	5.5743E-7	2.9974	3.1077E-4	1.9979	5.5712E-7	2.9967	3.1060E-4	1.9971

TABLE 4. Interpolation errors and convergence rates for cubic IFE spaces, $\beta_1 = 1$ and $\beta_2 = 5$.

	Normal extended jump conditions				Laplacian extended jump conditions			
h	$\|u - I_h u\|_{0,\Omega}$	rate	$\|u - I_h u\|_{1,\Omega}$	rate	$\|u - I_h u\|_{0,\Omega}$	rate	$\|u - I_h u\|_{1,\Omega}$	rate
1/10	8.1195E-5	NA	4.5877E-3	NA	7.9335E-5	NA	4.5483E-3	NA
1/20	5.0095E-6	4.0187	5.7954E-4	2.9848	4.9670E-6	3.9975	5.7467E-4	2.9845
1/40	3.1393E-7	3.9962	7.2864E-5	2.9916	3.1292E-7	3.9885	7.2793E-5	2.9809
1/80	1.9655E-8	3.9975	9.1648E-6	2.9910	1.9721E-8	3.9880	9.1907E-6	2.9855
1/160	1.2286E-9	3.9998	1.1504E-6	2.9939	1.2274E-9	4.0060	1.2252E-6	2.9072

TABLE 5. Interpolation errors and convergence rates for quadratic IFE spaces, $\beta_1 = 1$ and $\beta_2 = 100$.

	Normal extended jump conditions				Laplacian extended jump conditions			
h	$\|u - I_h u\|_{0,\Omega}$	rate	$\|u - I_h u\|_{1,\Omega}$	rate	$\|u - I_h u\|_{0,\Omega}$	rate	$\|u - I_h u\|_{1,\Omega}$	rate
1/10	7.3534E-4	NA	2.7176E-2	NA	1.2661E-3	NA	4.6494E-2	NA
1/20	9.3163E-5	2.9806	6.6039E-3	2.0410	9.6655E-5	3.7115	6.8429E-3	2.7644
1/40	1.2454E-5	2.9031	1.7455E-3	1.9196	1.6740E-5	2.5295	2.5419E-3	1.4287
1/80	1.6313E-6	2.9325	4.5476E-4	1.9405	4.7763E-6	1.8093	1.3870E-3	0.8740
1/160	2.0823E-7	2.9692	1.1615E-4	1.9691	3.5992E-7	3.7301	2.1084E-4	2.7177

TABLE 6. Interpolation errors and convergence rates for cubic IFE spaces, $\beta_1 = 1$ and $\beta_2 = 100$.

	Normal extended jump conditions				Laplacian extended jump conditions			
h	$\|u - I_h u\|_{0,\Omega}$	rate	$\|u - I_h u\|_{1,\Omega}$	rate	$\|u - I_h u\|_{0,\Omega}$	rate	$\|u - I_h u\|_{1,\Omega}$	rate
1/10	5.0669E-5	NA	2.9256E-3	NA	1.0067E-4	NA	5.7367E-3	NA
1/20	3.3035E-6	3.9391	3.8481E-4	2.9265	2.3124E-5	2.1221	2.3970E-3	1.2590
1/40	2.1864E-7	3.9173	5.0583E-5	2.9274	6.5877E-7	5.1335	1.4324E-4	4.0647
1/80	1.4273E-8	3.9372	6.5889E-6	2.9405	3.9673E-8	4.0536	1.6768E-5	3.0947
1/160	8.6548E-10	4.0437	8.0725E-7	3.0290	2.2662E-9	4.1298	1.9795E-6	3.0825

We present numerical results for three interface problems to demonstrate the approximation capabilities of the p-th degree IFE spaces constructed by the least squares method. The exact solution to the first problem satisfies both extended jump conditions. The exact solution to the second problem satisfies extended Laplacian extended jump conditions but not the normal extended jump condition. Finally, the exact solution to the last problem satisfies neither extended interface conditions. We will test both the moderate and large mismatch ratio β_1/β_2. We construct the shape functions by selecting the weights $\omega_0 = \max(\beta_1, \beta_2)^2$ and $\omega_j = |\Gamma \cap T|^{2j}$, $j = 1, 2, \ldots, p$, in the bilinear forms (13) and (14). The parameters in (12) are chosen such that $k_1 = 0.1$ and $k_2 = 2$. We will also use $\epsilon = -1$ and $\sigma_e^0 = 30$ in the symmetric partially penalized (SPP) IFE method.

3.1. Example 1. The domain is $\Omega = (-1, 1) \times (-1, 1)$ and the interface Γ is the circle with radius $r_0 = \pi/6.28$ which divides Ω into two subdomains Ω^1 and Ω^2 with

$$\Omega^1 = \{(x, y) : x^2 + y^2 < r_0^2\}.$$

Functions f and g in the interface problem (1) are such that its exact solution is

$$u(x,y) = \begin{cases} \dfrac{1}{\beta_1} r^\alpha, & (x,y) \in \Omega^1, \\ \dfrac{1}{\beta_2} r^\alpha + \left(\dfrac{1}{\beta_1} - \dfrac{1}{\beta_2}\right) r_0^\alpha, & (x,y) \in \Omega^2, \end{cases} \tag{35}$$

where $r = \sqrt{x^2 + y^2}$ and $\alpha = 5$.

The errors and convergence rates of the IFE interpolation of u are presented in Tables 3-6 which suggest an optimal convergence. The errors and convergence rates of the IFE solution to the interface problem are in Tables 7-8 which also suggest an optimal convergence. We expect the p-th degree IFE spaces constructed by the least squares method using either the normal or the Laplacian extended jump conditions to perform optimally because the exact solution u in this example satisfies both normal and Laplacian extended interface conditions.

TABLE 7. Errors in SPP quadratic IFE solution and convergence rates, $\beta_1 = 1$ and $\beta_2 = 5$.

	Normal extended jump conditions				Laplacian extended jump conditions			
h	$\|u-u_h\|_{0,\Omega}$	rate	$\|u-u_h\|_{1,\Omega}$	rate	$\|u-u_h\|_{0,\Omega}$	rate	$\|u-u_h\|_{1,\Omega}$	rate
1/10	2.2362E-3	NA	7.8165E-2	NA	2.2341E-3	NA	7.7892E-2	NA
1/20	2.8245E-4	2.9850	1.9671E-2	1.9905	2.8241E-4	2.9839	1.9679E-2	1.9848
1/40	3.5522E-5	2.9912	4.9500E-3	1.9905	3.5518E-5	2.9912	4.9490E-3	1.9914
1/80	4.4535E-6	2.9957	1.2410E-3	1.9959	4.4529E-6	2.9858	1.2407E-3	1.9959
1/160	5.5758E-7	2.9977	3.1077E-4	1.9976	5.5771E-7	2.9972	3.1081E-4	1.9971

TABLE 8. Errors in SPP quadratic IFE solution and convergence rates, $\beta_1 = 1$ and $\beta_2 = 100$.

	Normal extended jump conditions				Laplacian extended jump conditions			
h	$\|u-u_h\|_{0,\Omega}$	rate	$\|u-u_h\|_{1,\Omega}$	rate	$\|u-u_h\|_{0,\Omega}$	rate	$\|u-u_h\|_{1,\Omega}$	rate
1/10	7.3758E-4	NA	2.4944E-2	NA	7.4924E-4	NA	2.5166E-2	NA
1/20	9.5883E-5	2.9435	6.5378E-3	1.9318	1.0019E-4	2.9027	6.7053E-3	1.9081
1/40	1.2955E-5	2.8878	1.7650E-3	1.8892	1.3483E-5	2.8935	1.8146E-3	1.8856
1/80	1.6643E-6	2.9605	4.5616E-4	1.9520	1.7003E-6	2.9873	4.6318E-4	1.9700
1/160	2.1041E-7	2.9836	1.1573E-4	1.9788	2.1350E-7	2.9935	1.1692E-4	1.9860

TABLE 9. Interpolation errors and convergence rates for quadratic IFE spaces.

	Small jump: $\beta_1 = 1$ and $\beta_2 = 5$				Larger jump: $\beta_1 = 1$ and $\beta_2 = 100$			
h	E1*	rate	E2**	rate	E1	rate	E2	rate
1/10	1.1645E-1	NA	6.5212E-0	NA	8.4099E-3	NA	7.8720E-1	NA
1/20	1.7706E-2	2.7174	1.9532E-0	1.7393	1.5398E-3	2.4493	2.7782E-1	1.5026
1/40	2.4360E-3	2.8617	5.3366E-1	1.8719	2.1407E-4	2.8466	5.7528E-2	2.2718
1/80	3.1928E-4	2.9316	1.3942E-1	1.9365	2.8345E-5	2.9169	1.4938E-2	1.9453
1/160	4.0862E-5	2.9660	3.5626E-2	1.9684	4.1645E-6	2.7669	4.0999E-3	1.8654

*E1 denotes $\|u - I_h u\|_{0,\infty,\Omega}$, **E2 denotes $|u - I_h u|_{1,\infty,\Omega}$.

Tables 9-10 present errors of IFE interpolations gauged in the L^∞ and semi-$H^{1,\infty}$ norms from which we can see that the quadratic IFE spaces have an almost optimal convergence rate in the L^∞ and semi-$H^{1,\infty}$ norms. However, we observe that errors in cubic IFE interpolations in the L^∞ norm behave optimally when the ratio of β_1 and β_2 is small, but the convergence rate deteriorate in other cases listed in Table 10 as the mesh becomes finer.

TABLE 10. Interpolation errors and convergence rates for cubic IFE spaces.

	Small jump: $\beta_1 = 1$ and $\beta_2 = 5$				Larger jump: $\beta_1 = 1$ and $\beta_2 = 100$			
h	E1	rate	E2	rate	E1	rate	E2	rate
1/10	6.7911E-3	NA	4.3699E-1	NA	1.8308E-3	NA	2.8334E-1	NA
1/20	4.8461E-4	3.8087	6.2825E-2	2.7982	1.2023E-4	3.9286	3.2052E-2	3.1440
1/40	3.2316E-5	3.9065	8.4064E-3	2.9018	8.0001E-6	3.9096	3.4944E-3	3.1973
1/80	2.0855E-6	3.9538	1.0867E-3	2.9515	7.7950E-7	3.3594	3.3271-3	0.0708
1/160	1.3242E-7	3.9772	1.5603E-3	-0.5219	1.3537E-6	-0.7963	1.1712E-2	-1.8157

*E1 denotes $\|u - I_h u\|_{0,\infty,\Omega}$, **E2 denotes $|u - I_h u|_{1,\infty,\Omega}$.

3.2. Example 2. The second problem is on $\Omega = (0.6, 1.6) \times (0.21, 1.21)$ cut by interface Γ given as

$$\Gamma = \{(x, y), \mid L(x, y) := (x^2 - y^2)^2 - 4x^2y^2 + 0.5 = 0\},$$

where $L(x, y)$ is a harmonic polynomial whose conjugate is $\overline{L}(x, y) = 4xy(x^2 - y^2)$. As illustrated in Figure 12, Ω is split into

$$\Omega^1 = \{(x, y) \in \Omega : L(x, y) < 0\}, \text{ and } \Omega^2 = \{(x, y) \in \Omega : L(x, y) > 0\}.$$

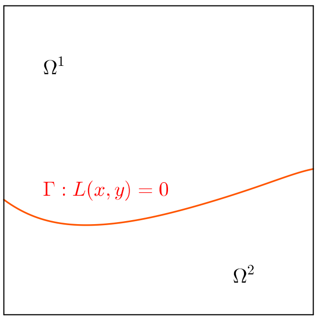

FIGURE 12. The domain and interface for Example 2.

Since $\triangle\overline{L} = 0$ and $\nabla L \cdot \nabla\overline{L} = 0$ for all x, y, we can let $f = 0$ and choose g to be such that the exact solution to the interface problem (1) is

$$u(x, y) = \begin{cases} \dfrac{\overline{L}(x, y) - \beta_2 L(x, y)}{\beta_2 - \beta_1}, & (x, y) \in \Omega^1, \\ \dfrac{\overline{L}(x, y) - \beta_1 L(x, y)}{\beta_2 - \beta_1}, & (x, y) \in \Omega^2. \end{cases} \tag{36}$$

Note that u in this example has a nonzero tangential derivative along the interface Γ. Furthermore, it can be verified that u given in (36) satisfies the Laplacian extended jump conditions but not the normal extended jump conditions.

TABLE 11. Interpolation errors and convergence rates for quadratic IFE spaces, $\beta_1 = 1$ and $\beta_2 = 5$.

	Normal extended jump conditions				Laplacian extended jump conditions			
h	$\|u - I_h u\|_{0,\Omega}$	rate	$\|u - I_h u\|_{1,\Omega}$	rate	$\|u - I_h u\|_{0,\Omega}$	rate	$\|u - I_h u\|_{1,\Omega}$	rate
1/10	3.0924E-4	NA	3.2368E-2	NA	2.6032E-4	NA	2.9839E-2	NA
1/20	4.4250E-5	2.8050	8.9578E-3	1.8534	3.2632E-5	2.9960	7.4757E-3	1.9969
1/40	6.4364E-6	2.7813	2.5053E-3	1.8382	4.0776E-6	3.0005	1.8700E-3	1.9992
1/80	1.0274E-6	2.6473	7.5982E-4	1.7213	5.0996E-7	2.9993	4.6768E-4	1.9994
1/160	1.7708E-7	2.5366	2.5043E-4	1.6012	6.3761E-8	2.9996	1.1694E-4	1.9997

TABLE 12. Interpolation errors and convergence rates for quadratic IFE spaces, $\beta_1 = 1$ and $\beta_2 = 5$.

	Normal extended jump conditions				Laplacian extended jump conditions			
h	$\|u - I_h u\|_{0,\Omega}$	rate	$\|u - I_h u\|_{1,\Omega}$	rate	$\|u - I_h u\|_{0,\Omega}$	rate	$\|u - I_h u\|_{1,\Omega}$	rate
1/10	4.8270E-5	NA	3.2368E-2	NA	1.5597E-6	NA	1.5958E-4	NA
1/20	7.4538E-6	2.6951	8.9578E-3	1.6807	9.7688E-8	3.9969	2.0065E-5	2.9939
1/40	1.6712E-6	2.1571	2.5053E-3	1.2261	6.0741E-9	4.0074	2.5014E-6	3.0006
1/80	2.9106E-7	2.5215	2.9137E-4	1.5500	3.7884E-10	4.0030	3.1185E-7	3.0011
1/160	5.0069E-8	2.5393	1.0084E-4	1.5308	8.4674E-11	2.1616	4.0914E-8	2.9561

Interpolation errors and convergence rates are presented in Tables 11-12. Data in the left two columns of Tables 11-12 show a suboptimal convergence for the IFE spaces constructed by the normal extended jump conditions. On the other hand, results in the last two columns of Tables 11-12 suggest that the IFE spaces constructed by the Laplacian extended jump conditions have the expected optimal approximation capability even though the convergence rates degenerate a little which, we think, might be the consequence of round-off error. These numerical results clearly demonstrate that the performance of an IFE space cannot be guaranteed to be optimal if it is not constructed according to the extended jump conditions suitable to the exact solution.

The data in Tables 13 demonstrate that numerical solutions generated from the 2nd degree IFE space constructed according to the Laplacian extended jump conditions can converge optimally. We omit results for IFE solutions satisfying the normal extended jump conditions, but we simply report that they converge sub-optimally as suggested by their interpolation counterparts.

TABLE 13. Errors in SPP quadratic IFE solution and convergence rates.

	Small jump: $\beta_1 = 1$ and $\beta_2 = 5$				Larger jump: $\beta_1 = 1$ and $\beta_2 = 100$			
h	$\|u - u_h\|_{0,\Omega}$	rate	$\|u - u_h\|_{1,\Omega}$	rate	$\|u - u_h\|_{0,\Omega}$	rate	$\|u - u_h\|_{1,\Omega}$	rate
1/10	2.6606E-4	NA	2.9916E-2	NA	2.1344E-4	NA	2.3661E-2	NA
1/20	3.2899E-5	3.0156	7.4860E-3	1.9986	2.6256E-5	3.0231	5.8785E-3	2.0090
1/40	4.0987E-6	3.0048	1.8709E-3	2.0004	3.2064E-6	3.0336	1.4629E-3	2.0066
1/80	5.1160E-7	3.0021	4.6783E-4	1.9997	4.0003E-7	3.0028	3.6559E-4	2.0005
1/160	6.3882E-8	3.0015	1.1696E-4	1.9999	4.9878E-8	3.0036	9.1327E-5	2.0011

3.3. Example 3. The domain is $\Omega = (-1.21, 1.21) \times (-1.21, 1.21)$ cut by the circular interface $\Gamma = \{(x, y) \mid x^2 + y^2 = 1\}$ which split Ω into $\Omega^1 = \{(x, y) \in \Omega : x^2 + y^2 < 1\}$ and $\Omega^2 = \{(x, y) \in \Omega : x^2 + y^2 > 1\}$. Function f and g in the interface problem (1) are such that its exact solution is

$$u(x,y) = \begin{cases} 1+\pi-\sqrt{2}\cos\Big(\dfrac{\pi}{4}(x^2+y^2)\Big), & (x,y)\in\Omega^1, \\ \pi\sqrt{x^2+y^2}, & (x,y)\in\Omega^2, \end{cases} \tag{37}$$

which satisfies (1a)-(1d) with $\beta_1 = 2$ and $\beta_2 = 1$. However, the true solution u fails to satisfy both normal and Laplacian extended jump conditions.

First, we note that data in Tables 14 show that the linear IFE space discussed in [16] that does not need extended jump conditions performs optimally for the interface problem in this example. On the other hand, data in Tables 15-16 indicate that approximations generated from higher degree IFE spaces can only perform sub-optimally. Again, this example suggests that it is critical to construct an IFE space according to the interface problem to be solved; otherwise, the optimal convergence cannot be certain.

TABLE 14. Errors and convergence rates for linear IFE interpolation and SPPG linear IFE solution, $\beta_1 = 2$ and $\beta_2 = 1$.

	Interpolation errors				SPP IFE solution error			
h	$\|u-u_h\|_{0,\Omega}$	rate	$\|u-u_h\|_{1,\Omega}$	rate	$\|u-u_h\|_{0,\Omega}$	rate	$\|u-u_h\|_{1,\Omega}$	rate
1/10	5.3665E-2	NA	5.8557E-1	NA	4.3372E-2	NA	5.0108E-1	NA
1/20	1.2910E-2	2.0554	2.8597E-1	1.0340	1.2029E-2	1.8503	2.4957E-1	1.0056
1/40	3.1817E-3	2.0207	1.4285E-1	1.0013	3.0693E-3	1.9705	1.2449E-1	1.0034
1/80	7.9375E-4	2.0030	7.1348E-2	1.0016	7.5360E-4	2.0260	6.2369E-2	0.9971
1/160	1.9827E-4	2.0012	3.5694E-2	0.9992	1.8922E-4	1.9937	3.1133E-2	1.0026

TABLE 15. Errors and convergence rates for interpolation and SPPG solution with quadratic IFE functions based on the normal extended jump conditions, $\beta_1 = 2$ and $\beta_2 = 1$.

	Interpolation errors				SPP IFE solution error			
h	$\|u-u_h\|_{0,\Omega}$	rate	$\|u-u_h\|_{1,\Omega}$	rate	$\|u-u_h\|_{0,\Omega}$	rate	$\|u-u_h\|_{1,\Omega}$	rate
1/10	3.9159E-3	NA	1.1378E-1	NA	2.6490E-3	NA	7.7531E-2	NA
1/20	7.8277E-4	2.3227	4.3396E-2	1.3907	5.0119E-4	2.4020	2.9562E-2	1.3910
1/40	1.1081E-4	2.8205	1.2980E-2	1.7412	1.0827E-4	2.2107	1.2296E-2	1.2655
1/80	2.3265E-5	2.2519	5.1928E-3	1.3217	1.6749E-5	2.6925	3.9101E-3	1.6529
1/160	3.6762E-6	2.6619	1.6949E-2	1.6153	2.9914E-6	2.4852	1.3942E-3	1.4877

TABLE 16. Errors and convergence rates for interpolation and SPPG solution with quadratic IFE functions based on the Laplacian extended jump conditions, $\beta_1 = 2$ and $\beta_2 = 1$.

	Interpolation errors				SPP IFE solution error			
h	$\|u-u_h\|_{0,\Omega}$	rate	$\|u-u_h\|_{1,\Omega}$	rate	$\|u-u_h\|_{0,\Omega}$	rate	$\|u-u_h\|_{1,\Omega}$	rate
1/10	3.8069E-3	NA	1.1018E-1	NA	2.6546E-3	NA	8.1858E-2	NA
1/20	7.9083E-4	2.2672	4.3936E-2	1.3264	4.8616E-4	2.4490	2.9118E-2	1.4912
1/40	1.1116E-4	2.8307	1.2985E-2	1.7585	1.0352E-4	2.2315	1.1964E-2	1.2832
1/80	2.3373E-5	2.2498	5.2042E-3	1.3191	1.6326E-5	2.6647	3.8443E-3	1.6379
1/160	3.6838E-6	2.6656	1.6919E-3	1.6211	2.8871E-6	2.4995	1.3630E-3	1.4959

4. Conclusion

We have presented a general framework for constructing higher degree IFE spaces for solving curved interface problems. We have proved that such high-degree spaces exist and may be unique under some conditions on the interface curve. Through computations, we have also shown that the proposed IFE spaces associated with given extended jump conditions may possess an optimal approximation capability if the true solution and the IFE spaces satisfy the same extended jump conditions. Future work will include an error analysis to prove optimality of IFE spaces and an investigation of IFE spaces for problems with non-smooth interfaces.

References

[1] Slimane Adjerid, Mohamed Ben-Romdhane, and Tao Lin. Higher degree immersed finite element spaces constructed according to the actual interface (submitted, 2016).

[2] Slimane Adjerid, Mohamed Ben-Romdhane, and Tao Lin. Higher degree immersed finite element methods for second-order elliptic interface problems. Int. J. Numer. Anal. Model., 11(3):541–566, 2014.

[3] Slimane Adjerid and Tao Lin. A p-th degree immersed finite element for boundary value problems with discontinuous coefficients. Appl. Numer. Math., 59(6):1303–1321, 2009.

[4] Ivo Babuška. The finite element method for elliptic equations with discontinuous coefficients. Computing (Arch. Elektron. Rechnen), 5:207–213, 1970.

[5] John W. Barrett and Charles M. Elliott. Fitted and unfitted finite-element methods for elliptic equations with smooth interfaces. IMA J. Numer. Anal., 7(3):283–300, 1987.

[6] Mohamed Ben-Romdhane. Higher-degree immersed finite elements for second-rrder elliptic interface problems. PhD thesis, Virginia Polytechnic Institute and State University, 2011.

[7] Martin P. Bendsøe. Optimization of structural topology, shape, and material. Springer-Verlag, Berlin, 1995.

[8] Dietrich Braess. Finite elements. Cambridge University Press, Cambridge, second edition, 2001. Theory, fast solvers, and applications in solid mechanics, Translated from the 1992 German edition by Larry L. Schumaker.

[9] James H. Bramble and J. Thomas King. A finite element method for interface problems in domains with smooth boundaries and interfaces. Adv. Comput. Math., 6(2):109–138, 1996.

[10] Brian Camp, Tao Lin, Yanping Lin, and Weiwei Sun. Quadratic immersed finite element spaces and their approximation capabilities. Adv. Comput. Math., 24(1-4):81–112, 2006.

[11] Waixiang Cao, Xu Zhang, and Zhimin Zhang. Superconvergence of immersed finite element methods for interface problems. Advances in Computational Mathematics, 2017.

[12] Zhiming Chen and Jun Zou. Finite element methods and their convergence for elliptic and parabolic interface problems. Numer. Math., 79(2):175–202, 1998.

[13] Ray. W. Clough and James L. Tocher. Finite element stiffness matrices for analysis of plate bending. In Matrix Methods in Structual Mechanics, pages 515–545, 1966.

[14] Yan Gong, Bo Li, and Zhilin Li. Immersed-interface finite-element methods for elliptic interface problems with nonhomogeneous jump conditions. SIAM J. Numer. Anal., 46(1):472–495, 2007/08.

[15] Phillip Griffiths. Introduction to algebraic curves, volume 76.;76;. American Mathematical Society, Providence, R.I, 1989.

[16] Ruchi Guo and Tao Lin. A group of immersed finite element spaces for elliptic interface problems. arXiv:1612.00919, 2016.

[17] Ruchi Guo, Tao Lin, and Xu Zhang. Nonconforming immersed finite element spaces for elliptic interface problems. arXiv:1612.01862, 2016.

[18] Johnny Guzmán, Nanuel A. Sánchez, and Marcus Sarkis. A finite element method for high-contrast interface problems with error estimates independent of contrast. arXiv:1507.03873v3, 2016.

[19] Johnny Guzmán, Nanuel A. Sánchez, and Marcus Sarkis. Higher-order finite element methods for elliptic problems with interfaces. ESAIM: M2AN, 50(5):1561–1583, 2016.

[20] Johnny Guzmán, Nanuel A. Sánchez, and Marcus Sarkis. On the accuracy of finite element approximations to a class of interface problems. Mathematics of Computation, 85:2071–2098, 2016.

[21] Anita Hansbo and Peter Hansbo. An unfitted finite element method, based on Nitsche's method, for elliptic interface problems. Comput. Methods Appl. Mech. Engrg., 191(47-48):5537–5552, 2002.

[22] Jaroslav Haslinger and Pekka Neittaamäki. Finite element approximation for optimal shape, material and topology design. John Wiley & Sons, Ltd, Chichester, 1996.

[23] Xiaoming He. Bilinear immersed finite elements for interface problems. PhD thesis, Virginia Polytechnic Institute and State University, 2009.

[24] Xiaoming He, Tao Lin, and Yanping Lin. Approximation capability of a bilinear immersed finite element space. Numer. Methods Partial Differential Equations, 24(5):1265–1300, 2008.

[25] Xiaoming He, Tao Lin, and Yanping Lin. Interior penalty bilinear IFE discontinuous Galerkin methods for elliptic equations with discontinuous coefficient. J. Syst. Sci. Complex., 23(3):467–483, 2010.

[26] Daniel D. Joseph and Yuriko Y. Renardy. Fundamentals of two-fluid dynamics. Part I, volume 3 of Interdisciplinary Applied Mathematics. Springer-Verlag, New York, 1993. Mathematical theory and applications.

[27] Do Y. Kwak, Kye T. Wee, and Kwang S. Chang. An analysis of a broken P_1-nonconforming finite element method for interface problems. SIAM J. Numer. Anal., 48(6):2117–2134, 2010.

[28] Randall J. LeVeque and Zhi Lin Li. The immersed interface method for elliptic equations with discontinuous coefficients and singular sources. SIAM J. Numer. Anal., 31(4):1019–1044, 1994.

[29] Jie Li, Yuriko Renardy, and Michael Renardy. Numerical simulation of breakup of a viscous drop in simple shear flow through a volume-of-fluid method. Phys. Fluids, 12(2):269–282, 2000.

[30] Zhilin Li. The immersed interface method using a finite element formulation. Appl. Numer. Math., 27(3):253–267, 1998.

[31] Zhilin Li and Kazufumi Ito. The immersed interface method, volume 33 of Frontiers in Applied Mathematics. Society for Industrial and Applied Mathematics (SIAM), Philadelphia, PA, 2006. Numerical solutions of PDEs involving interfaces and irregular domains.

[32] Zhilin Li, Tao Lin, Yanping Lin, and Robert C. Rogers. An immersed finite element space and its approximation capability. Numer. Methods Partial Differential Equations, 20(3):338–367, 2004.

[33] Zhilin Li, Tao Lin, and Xiaohui Wu. New Cartesian grid methods for interface problems using the finite element formulation. Numer. Math., 96(1):61–98, 2003.

[34] Tao Lin, Yanping Lin, Robert Rogers, and M. Lynne Ryan. A rectangular immersed finite element space for interface problems. In Scientific computing and applications (Kananaskis, AB, 2000), volume 7 of Adv. Comput. Theory Pract., pages 107–114. Nova Sci. Publ., Huntington, NY, 2001.

[35] Tao Lin, Yanping Lin, and Weiwei Sun. Error estimation of a class of quadratic immersed finite element methods for elliptic interface problems. Discrete Contin. Dyn. Syst. Ser. B, 7(4):807–823, 2007.

[36] Tao Lin, Yanping Lin, and Xu Zhang. Partially penalized immersed finite element methods for elliptic interface problems. SIAM J. Numer. Anal., 53(2):1121–1144, 2015.

[37] Ralf Massjung. An unfitted discontinuous galerkin method applied to elliptic interface problems. SIAM Journal on Numerical Analysis, 50(6):3134–3162, 2012.

[38] Promode K. Saikia. Linear algebra. Pearson, New Delhi, India, 2009.

[39] Fei Wang, Yuanming Xiao, and Jinchao Xu. High-order extended finite element methods for solving interface problems. arXiv:1604.06171, 2016.

[40] Jinchao Xu. Estimate of the convergence rate of the finite element solutions to elliptic equation of second order with discontinuous coefficients. Natural Science Journal of Xiangtan University, 1:1–5, 1982.

[41] Xu Zhang. Nonconforming Immersed Finite Element Methods for Interface Problems. 2013. Thesis (Ph.D.)–Virginia Polytechnic Institute and State University.

Department of Mathematics, Virginia Tech
E-mail: adjerids@math.vt.edu, ruchi91@vt.edu, tlin@vt.edu